Reversible Interconversion of a Divalent Vanadium Bronze between δ and β Quasi-1D Structures

Peter M. Marley and Sarbajit Banerjee*

Department of Chemistry, University at Buffalo, State University of New York, Buffalo, New York 14260-3000, United States

ABSTRACT: Charge fluctuations along the quasi-1D frameworks of $M_xV_2O_5$ bronzes have evinced much recent interest owing to the manifestation of colossal metal−insulator transitions and superconductivity. Depending upon the nature of the intercalating cation (M), distinctive geometries of the V_2O_5 framework are accessible. Herein, we demonstrate an unprecedented reversible transformation between double-layered (δ) and tunnel (β) quasi-1D geometries for nanowires of a divalent vanadium bronze, $Ca_xV_2O_5$ ($x \approx 0.23$), upon annealing-induced dehydration and hydrothermally induced hydration. Such a facile hydration/dehydration-induced interconversion between two prominent quasi-1D structures (accompanied by a change in charge-ordering motifs) has not been observed in the bulk and is posited to result from the ease of propagation of crystallographic slip processes across the confined nanowire widths for the δ → β conversion and the facile diffusion of water molecules within the tunnel geometries for the β → δ reversion.
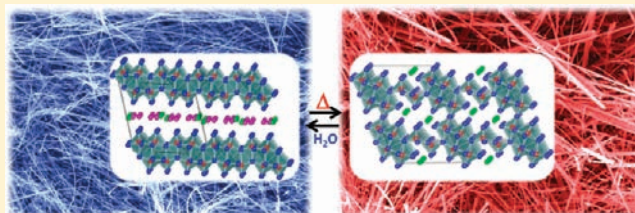
INTRODUCTION

The classical intercalation compound V_2O_5 comprises layers of $[VO_5]$ square pyramids sharing edges and corners and provides a robust and bountiful framework for exploration of intriguing charge-ordering motifs upon the insertion of guest cations.[1−7] Indeed, intercalative chemistry profoundly alters the structure and bonding of the layers and chains of vanadium-centered polyhedra facilitated primarily by crystallographic shear and slip and resulting in transformation of the simple orthorhombic layered structure to tunnel, double-layered, and more complex patterns.[8−10] Two especially notable commonalities of intercalated $M_xV_2O_5$ crystal structures are the propensity to adopt quasi-1D geometries and the complete ionization of the metal (M) cations located within tunnel and interstitial sites irrespective of their size and nature (common to alkali, alkaline-earth, and transition metal ions). The former has tremendous implications for electronic transport and confines carrier transport exclusively along the length of the tunnels or double layers (for instance, along the crystallographic b axis for the β and β′ phases and along the a axis for the δ phase).[11−14] The latter suggests a partial reduction of the host V_2O_5 framework and quasi-1D charge localization along the mixed-valence frameworks.

Quasi-1D charge localization can lead to the manifestation of dramatic Mott physics; indeed, $M_xV_2O_5$ bronzes can be considered to lie on the insulator side of a Mott transition with Coulomb repulsions giving rise to electron localization at specific framework sites along the tunnels/double layers.[12,14,15] In this regime, a thermally activated small polaron hopping mechanism allows for quasi-1D charge transport mediated by V−O−V square-pyramidal units. With increasing cation concentration, collective electron motion is induced along the length of the tunnels as metallic domains grow and coalesce,

engendering a stoichiometry-dependent metal−insulator transition.[6,7,11−13] The specific quasi-1D geometries and charge-ordering motifs depend upon the size and polarizability of the inserted cations. For instance, larger cations such as K^+ and Tl^+ crystallize in double-layered δ structures that can be thought to be derived from the layered V_2O_5 framework based on cation intercalation in alternate layers with inversion of some VO_5 square pyramids and slipping of adjacent layers (Figure 1a).[8] Another ubiquitous (and still quasi-1D) structure adopted by guest cations such as Na^+, Pb^{2+}, and Sr^{2+} is the tunnel bronze (β) phase depicted in Figure 1d. Vanadium atoms in the host framework are arrayed in three distinctive coordination environments, forming infinite chains or ladders extending along the crystallographic b axis and enclosing well-defined tunnels that are occupied by the guest cations. Smaller Li^+ or Cu^+ cations adopt a slightly different β′ crystal structure with essentially the same V_2O_5 framework as the β phase but with altered tunnel sites occupied by the cations (with a maximum occupancy $x \approx 0.66$). For Ag^+ and Ca^{2+}, both δ and β polymorphs are feasible, each with a distinctive charge-ordering and charge localization pattern. Herein, we report the first synthesis of nanostructures of the divalent vanadium bronze δ-$Ca_xV_2O_5 \cdot H_2O$ (with x approaching the stoichiometric limit of 0.25) and further evidence the hitherto unprecedented dehydration/hydration-induced reversible interconversion of δ and β phases.

Vanadium bronzes in all their fecundity have long attracted attention from solid-state chemists and physicists alike given the existence of strong electronic correlations and the intriguing commensurability physics derived from the mixed-valence
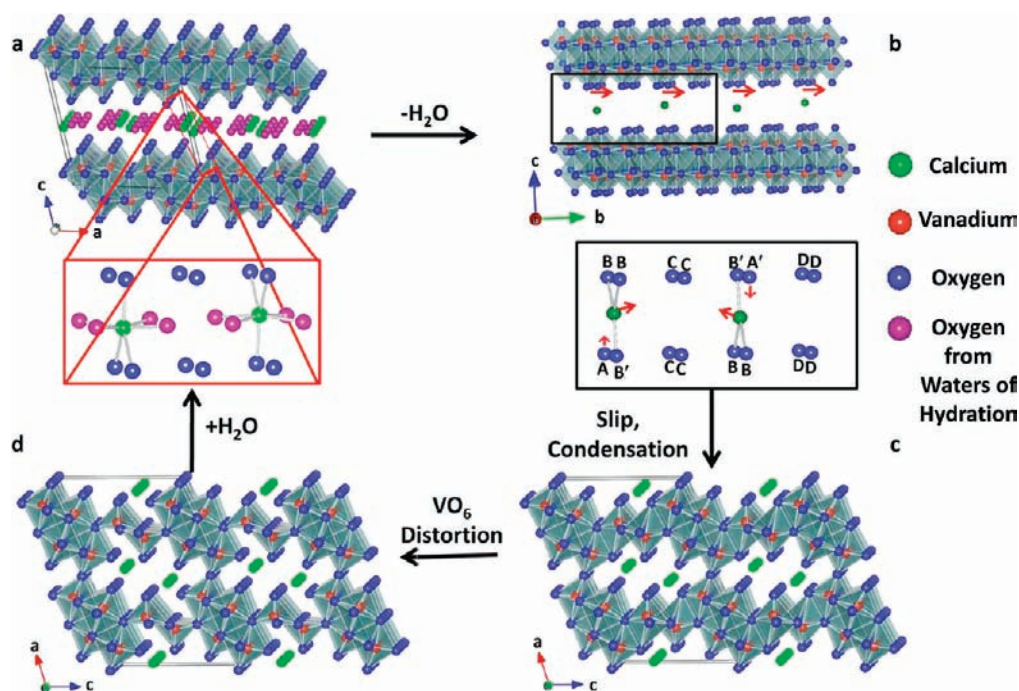
Figure 1. Schematic of the transformation from the hydrated δ phase to the tunnel-like β phase. (a) Crystal structure of δ-Ca$_x$V$_2$O$_5$·H$_2$O and a magnified portion of the calcium coordination environment illustrating the alternating calcium occupation corresponding to a maximum $x = 0.25$. Removal of interlayer water collapses the double layers (b), causing a slip, as shown by the red arrows; movement of the atoms is seen where O(A/A′) coordinate to the layers above and below through oxygen vacancies at O(D), and calcium ions coordinate to O(C) to yield the structure shown in (c). In (c) coordination of the layers through oxygen vacancies subsequent to the slip is shown. Distortion of the VO$_6$ octahedra coordinated to O(B′) and O(C) breaks a V—O bond, yielding VO$_5$ square pyramids, giving rise to the 1D tunnel framework of the β phase (d).

frameworks.[14,16−18] Wadsley et al. first examined the structure of β-Na$_x$V$_2$O$_5$ and demonstrated that the tunnel framework could accommodate a wide range of Na$^+$ compositions without any major deformations.[19] Sienko and co-workers predicted a doping-induced metal−insulator transition for Wadsley bronzes β-Na$_{0.33}$V$_2$O$_5$ and β-Li$_{0.33}$V$_2$O$_5$ based on extrapolations of measured magnetic susceptibilities and carrier mobilities.[15−18] However, only much later were Ueda and co-workers experimentally able to discern thermally induced metal−insulator phase transitions, albeit still only modest in magnitude, accompanied by charge ordering for these very same compounds.[5−7] These researchers determined that the magnitude of the phase transition exhibits great sensitivity to the precise stoichiometry (x in M$_x$V$_2$O$_5$), explaining the difficulties that previous researchers had in observing metal−insulator transitions in these materials. Of particular note, a superconducting phase adjacent to a charge-ordered phase has been reported by Ueda and co-workers in β-Na$_{0.33}$V$_2$O$_5$ and has inspired renewed interest in analogues of this compound, although no consensus has emerged regarding the optimal doping levels or charge-ordering patterns.[20]

In recent work, we have demonstrated that scaling to finite size enables the induction of colossal (up to 6 orders of magnitude) metal−insulator transitions in nanowires of δ-K$_{0.5}$V$_2$O$_5$ and β′-Cu$_{0.65}$V$_2$O$_5$.[12,13] The primary origin of this phenomenon is the establishment of precise cation stoichiometry along the tunnels and double-layered interstitial sites of M$_x$V$_2$O$_5$ nanostructures owing to the fortunate circumstance of "self-purification", which causes the migration of defects to the readily accessible surfaces of nanostructures. Elimination of random potentials arising from incomplete cation occupancies in tunnel/double-layered interstices ensures preservation of the

metallic character and allows the intrinsic electronic instabilities of these materials to be probed without obscuration from defect dynamics. Scaling to nanostructured dimensions further allows for tuning of the unusual concave phase diagrams of these materials,[6,7,20,21] enabling the metal−insulator transition temperature to be tuned up to room temperature and beyond. In related work, Zhang et al. have reported metal−insulator transitions for β-K$_{0.33}$V$_2$O$_5$ and Fe$_{2.5}$V$_{1.5}$OV$_{5.6}$O$_{16}$ nanostructures.[22,23] Herein, we provide the first evidence that the two distinctive quasi-1D polymorphs (δ and β) of a divalent vanadium bronze can be reversibly interconverted through thermal annealing and hydrothermal treatment (Figure 1). Notably, such a phase transformation has not been observed thus far in the bulk. While a detailed mechanistic understanding is not yet available, the facile interconversion evidenced here is clearly a consequence of the nanoscale dimensions, which enable the wieldy propagation of slip processes along the confined width of the nanostructures.

■ **EXPERIMENTAL SECTION**

Synthesis. δ-Ca$_x$V$_2$O$_5$·H$_2$O nanowires were prepared by ball milling stoichiometric amounts of Ca(NO$_3$)$_2$·4H$_2$O (J.T. Baker) or Ca(COOCH$_3$)$_2$·H$_2$O (Sigma-Aldrich) with V$_2$O$_5$ powder (Sigma-Aldrich 99.5%) in a Spex mill. The mixture was then placed in a Teflon cup and heated in a sealed autoclave (Parr) along with 16 mL of deionized water. The hydrothermal reaction was performed for 72 h at 250 °C. Upon cooling to room temperature, the product was vacuum filtered, washed with deionized water, and allowed to dry in air. The transformation to β-Ca$_x$V$_2$O$_5$ was performed under a 10^{-3} vacuum using a Schlenk line apparatus under various conditions as described below. The subsequent reversion of β-Ca$_x$V$_2$O$_5$ to δ-Ca$_x$V$_2$O$_5$·H$_2$O was achieved by hydrothermal treatment wherein ~300 mg of β-phase nanowires and 16 mL of deionized water were placed in a Teflon cup and heated in a sealed autoclave at 210 °C for 72 h.

Characterization. Powder X-ray diffraction (XRD) data were collected in Bragg–Brentano geometry using a Rigaku Ultima IV instrument (Cu Kα radiation, voltage 40 kV, current 44 mA). The nanowire samples were ground to a fine powder and packed in a sample holder with 0.5 mm depth for the powder XRD measurements. Pattern fitting and phase identification were achieved with the help of JADE 8.5. The morphology of the as-prepared nanowires was evaluated by scanning electron microscopy (SEM, Hitachi SU-70 operated at 25 kV equipped with an X-ray detector) and by combining high-resolution transmission electron microscopy (HRTEM) with selected area electron diffraction (SAED, JEOL-2010, 200 kV, 100 mA). For transmission electron microscopy, the samples were dispersed in 2-propanol using a bath sonicator and then deposited onto 300 mesh carbon-coated Cu grids. Differential scanning calorimetry (DSC, Q200 TA Instruments) measurements under a flowing nitrogen atmosphere were performed in the temperature range from 0 to 300 °C to study the phase transition. As-prepared nanowires were examined in the DSC experiments after being allowed to dry overnight in air at room temperature.

■ RESULTS AND DISCUSSION

Figure 1a depicts the crystal structure of the hydrothermally grown δ-Ca$_x$V$_2$O$_5$·H$_2$O phase. The δ phase crystallizes in the monoclinic C2/m space group with Ca^{2+} ions and water molecules occupying interlayer sites.[24,25] As noted above, the δ-Ca$_x$V$_2$O$_5$·H$_2$O phase can be conceptualized by starting with the open framework of V$_2$O$_5$, followed by insertion of metal cations between every other VO$_5$ layer. Subsequent compression and condensation of the double layers, followed finally by rotation of a square pyramid, and then combination of the layers yields the δ phase as pictured in Figure 1a.[8,25]

In δ-Ca$_x$V$_2$O$_5$·H$_2$O, Ca^{2+} ions along with water molecules reside between the vanadium-centered polyhedral layers; the water molecules hydrate the Ca^{2+} ions in solution and as depicted in the magnified inset in Figure 1a remain coordinated to the calcium ions between the V$_2$O$_5$ layers. The immediate coordination environment of the Ca^{2+} ions is constituted from a total of seven oxygen atoms, four derived from the waters of hydration and three from the V$_2$O$_5$ layers above and below; the 7-fold coordination of Ca^{2+} ions results in every alternate cation site of the δ phase being occupied along the b axis, thereby giving rise to a maximum stoichiometry of x = 0.25.

Figure 2a shows a powder XRD pattern of the as-prepared nanowires, which can be clearly indexed to phase-pure δ phase Ca$_{0.24}$V$_2$O$_5$·H$_2$O (Joint Committee of Powder Diffraction Standards (JCPDS) #88-0579); energy dispersive X-ray (EDX) spectroscopy data yield x = 0.23, very close to the stoichiometric limit of 0.25 for δ-Ca$_x$V$_2$O$_5$·H$_2$O. Considerable preferential orientation is observed with pronounced intensities of the (001), (003), (004), and (005) reflections. Figure 2b–d depicts powder XRD patterns acquired after thermally annealing the as-prepared nanowire samples, which are discussed in further detail below.

The SEM image in Figure 3a and the low-magnification TEM image shown in the inset depict the morphology and purity of hydrated δ-Ca$_x$V$_2$O$_5$ nanowires obtained by our hydrothermal process. The nanowires are single crystalline, as indicated by the lattice-resolved HRTEM image in Figure 3c and the clearly defined individual spots in the $[1\bar{1}2]$ zone axis SAED pattern (inset in Figure 3c). The SAED pattern can also be indexed to δ-Ca$_{0.24}$V$_2$O$_5$·H$_2$O (JCPDS #88-0579) and remains consistent along the length of the nanowire, corroborating their single-crystalline nature. The lattice-resolved HRTEM image indicates the a axis is parallel to the length of the nanowire with lattice spacings of 0.564 and 0.336
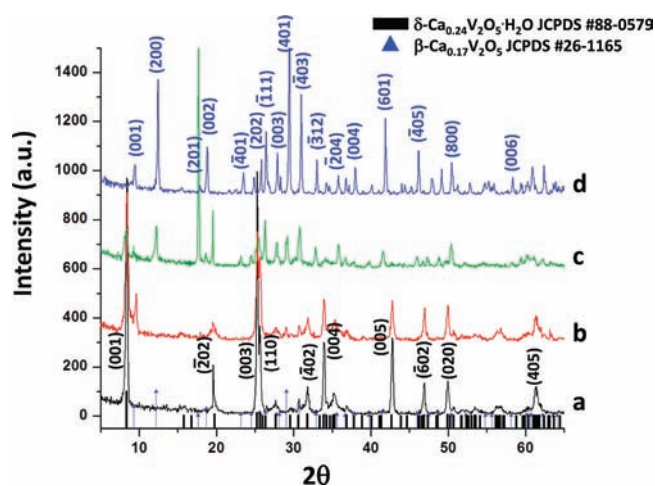
Figure 2. (a) XRD pattern of the as-prepared δ-phase nanowires. (b) Nanowires heated at 275 °C for 2 h. (c) As-prepared nanowires heated at 350 °C for 3 days. (d) Nanowires heated at 500 °C for 3 days indicating transformation to the β phase.

nm, corresponding to the separations between ($\bar{2}$01) and ($\bar{1}$11) planes, respectively. On the basis of the analysis of 50 nanowires, the nanowires upon reaction for 72 h at 210 °C have an average diameter of ∼207 nm and do not show an appreciable change in dimensions upon increasing the reaction time (Figure 3d).

The hydrated δ-phase nanowires have been carefully annealed, as indicated in Figure 2b–d. Upon heating δ-phase samples under vacuum for the appropriate amount of time to 500 °C, the transformation of δ-Ca$_x$V$_2$O$_5$·H$_2$O to phase-pure β-Ca$_x$V$_2$O$_5$ is evidenced without appreciable sintering of the nanostructures (Figure 2). At lower temperatures, the clear phase coexistence of β and δ phases is observed. For instance, upon heating the as-prepared nanowires to 275 °C for 2 h (Figure 2b), a broadening of the (001) reflection is evident along with the appearance of a new reflection at $2\theta = 9°$ corresponding to the (001) reflection of β-Ca$_x$V$_2$O$_5$. The broadening of the (001) reflection is likely due to the removal of interlayer water, which initiates collapse of the double-layered δ-phase structure (Figure 1b). Consistent with this feature, the (003) reflection of the δ phase is also seen to decrease upon heating, which is again explicable upon considering the removal of interlayer water. Phase coexistence of δ and β structures is still observed upon thermal annealing of the structures at 350 °C for 3 days; at this point, the intensity of the (001) reflection of the δ phase is greatly diminished and the (200) reflection of the β phase grows in intensity. The appearance of the (200) reflection suggests recrystallization of the collapsed VO$_6$ layers to form the incipient tunnel framework of the β phase. The reflection at $2\theta \approx 18°$ in Figure 2c coincides with the (201) reflection of the β phase, which is suggestive of condensation of the double layers. Unequivocal indexing of this reflection is precluded by the mixture of different phases present in this sample. Following the distortion and breaking of the V–O bond to complete the transformation to the β phase, the intensity of this reflection is greatly diminished. After annealing at 500 °C for 3 days, the as-prepared nanowires are completely transformed to β-Ca$_x$V$_2$O$_5$ (JCPDS #26-1165, Figure 2d).

Figure 4 shows a DSC profile of the as-prepared hydrated δ-phase nanowires indicating two distinctive peaks; the first more
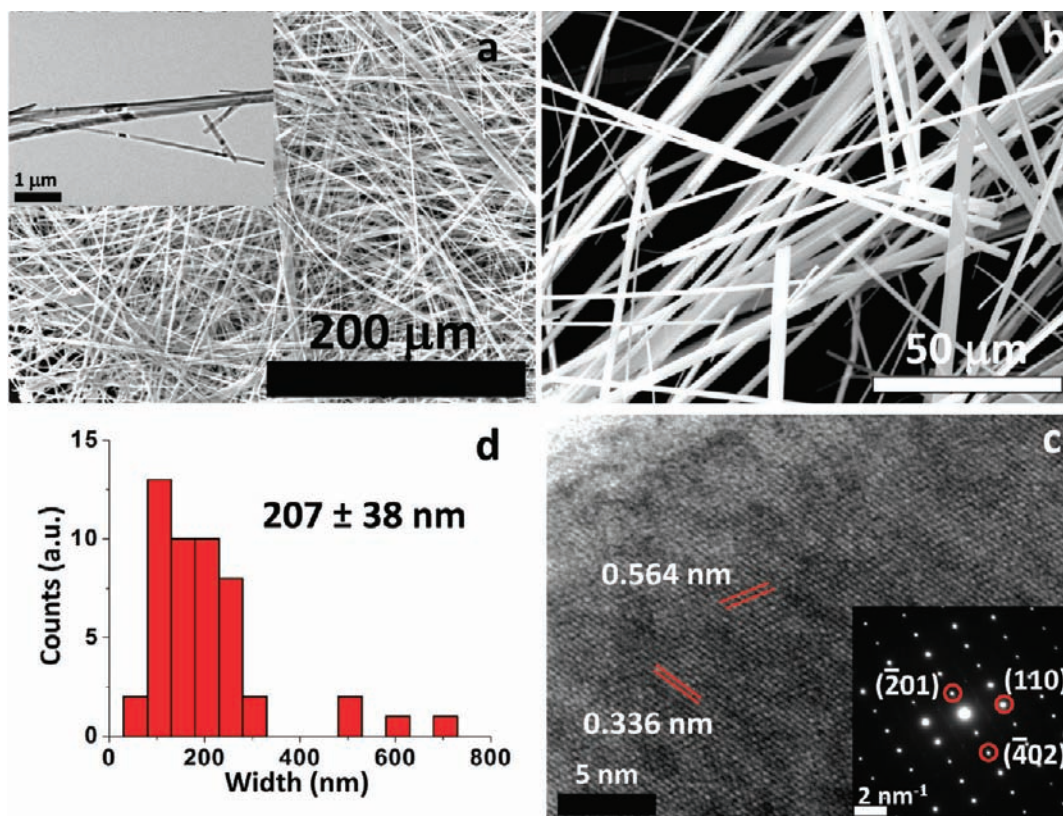
Figure 3. (a) Panoramic SEM image of the as-prepared δ-Ca$_x$V$_2$O$_5$·H$_2$O nanowires indicating the high yield and hundreds of micrometer lengths of the nanowires. A low-magnification TEM image of several nanowires is shown in the inset. (b) HRSEM image of multiple nanowires. (c) Lattice-resolved HRTEM image and SAED (inset) illustrating the single-crystalline nature of the nanowires. (d) Histogram deduced by measuring the lateral dimensions of 50 nanowires, indicating a size distribution centered at ∼207 nm.
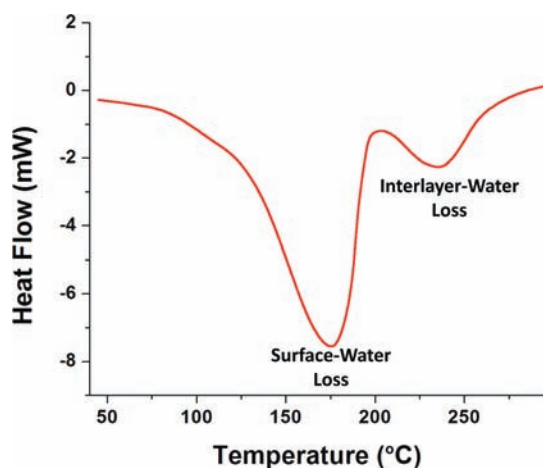
Figure 4. DSC trace measured for the as-prepared δ-Ca$_x$V$_2$O$_5$·H$_2$O nanowires. The first pronounced feature (∼175 °C) corresponds to surface water loss. The second peak (∼230 °C) arises from water loss from interstitial sites and initiation of structural rearrangement.

pronounced feature at ∼175 °C arises from loss of surface water from the nanowires. On the basis of data for an analogous hydrated barium vanadate compound, the broader, higher temperature feature at ∼230 °C can be attributed to removal of internal water occupying the interstitial space between the V$_2$O$_5$ double layers.[26] The DSC trace thus indicates that irreversible deintercalation of water molecules and collapse of the double layers are initiated around 230 °C, which is further consistent with the XRD pattern shown in Figure 2b. However,

complete rearrangement and recrystallization of the double layers to the β phase requires a temperature of 500 °C (Figure 2d).

Electron microscopy examination of the dehydrated β phase indicates the remarkable preservation of the anisotropic 1D nanowire morphology (Figure 5). The nanowires appear to have been cleanly transformed without fragmentation into smaller particles. The size distribution histogram in Figure 5d suggests an average diameter of ∼216 nm, which corresponds closely to that of the δ phase, indicating that there is no substantial sintering of the nanowires even at an annealing temperature of 500 °C. The lattice-resolved HRTEM image in Figure 5c indicates a spacing of 0.953 nm, which corresponds to the separation between (001) planes of the β phase and suggests that the b axis is parallel to the length of the nanowire. EDX analysis indicates a retention of the approximately $x \approx$ 0.23 stoichiometry, which is undersaturated for the β phase (a cation stoichiometry of $x \approx 0.33$ is required for observation of the correlated metallic phase).

The transformation of a single-layered ε-phase vanadium oxide bronze to the β phase has been conceptually examined by Galy et al. and is posited to involve shear slips of the single VO$_5$ layers into smaller sheets, which subsequently undergo reconstruction to form double layers of VO$_6$ octahedra followed by subsequent association by corner sharing to obtain the β phase.[9] The transformation of the double-layered δ phase to the β structure can follow a similar rearrangement pattern initiated by the removal of stabilizing interlayer water molecules, which causes collapse of the double layers (as illustrated in Figure 1b). Crystallographic slip of alternating
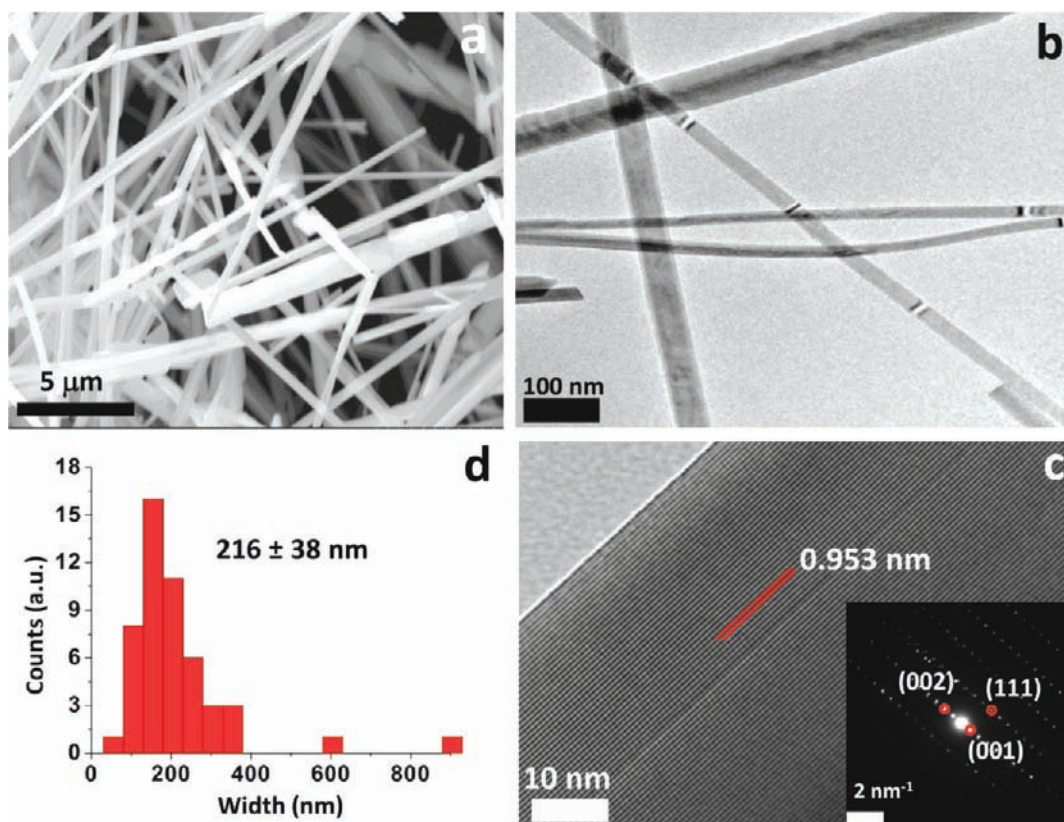
Figure 5. (a) SEM image of the nanowires heated to 500 °C for 3 days. (b) Low-magnification TEM image of several nanowires. (c) Lattice-resolved HRTEM image of the heated nanowires depicting the b axis is parallel to the length of the nanowire. A SAED shown in the inset can be indexed to β-Ca$_x$V$_2$O$_5$ (JCPDS #26-1165). (d) Width distribution of the nanowires deduced from the TEM images, indicating little change occurs upon heating.
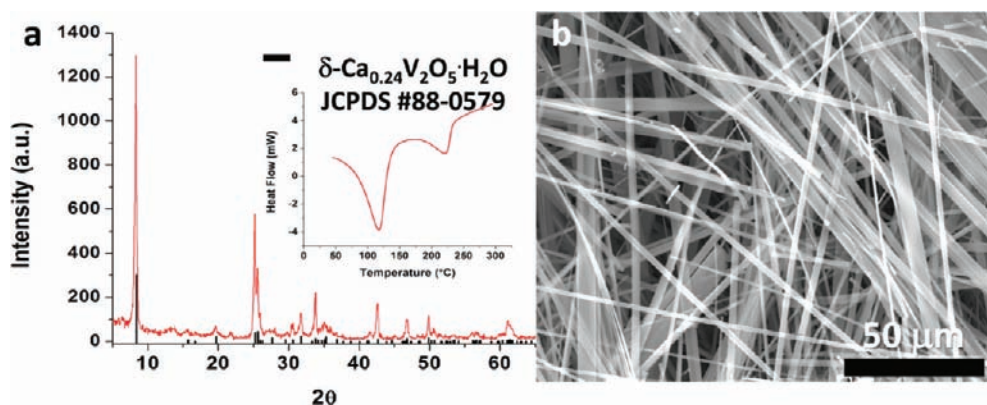
Figure 6. (a) XRD pattern of materials recovered by hydrothermal treatment of β-Ca$_x$V$_2$O$_5$ nanowires. The pattern can be indexed to the hydrated δ phase, showing the reversible nature of the phase transformation. The inset is a DSC trace of the rehydrated nanowires. (b) SEM image of δ-Ca$_x$V$_2$O$_5$ nanowires after rehydration from the β phase.

vanadium oxide layers as indicated by the red arrows in Figure 1b allows for the double layers to be correctly oriented for subsequent condensation along the c axis (defined with respect to the δ phase). The change in the local coordination environment of the intercalated Ca^{2+} ions is illustrated in the inset to Figure 1b. With removal of H$_2$O, the Ca^{2+} ions can be conceptualized as being pushed together as the V$_2$O$_5$ layers slip and condense. This allows for the Ca^{2+} ions to coordinate to the oxide ions denoted as C in the V$_2$O$_5$ framework. Subsequent association of the layers through oxygen sites (A/A' and D) through vacancies coordinates the VO$_6$ layers to form a tunnel-like structure (Figure 1c). Distortion of

vanadium-centered [VO$_6$] polyhedra connected to oxide ions C and B' results in a breaking of a V−O bond, yielding VO$_5$ square pyramids arrayed along the walls of the β phase (Figure 1d). Consequently, upon dehydration and nucleation of the β phase, the reconstruction can propagate facilely along the width of the nanowires without substantial alteration of the width distribution (Figure 5d) of the β-Ca$_x$V$_2$O$_5$ nanowires.

The reversible nature of the dehydration-induced $\delta \rightarrow \beta$ transformation is seen upon hydrothermal treatment of the β-Ca$_x$V$_2$O$_5$ nanowires. Upon hydrothermal treatment at 210 °C for 72 h, the β-Ca$_x$V$_2$O$_5$ nanowires revert back to hydrated δ-phase nanowires, as indicated by the powder diffraction pattern

in Figure 6a. Such a hydration-induced phase transformation has not been evidenced upon simple immersion of the β-$Ca_xV_2O_5$ nanowires in water or upon refluxing. The high autogenously generated pressure of hydrothermal reactions is thus clearly pivotal for enabling water molecules to enter the tunnel framework of the β phase, which subsequently exfoliates to re-form the layered δ-phase nanowires (Figure 6b). The inset in Figure 6a shows a DSC trace of the rehydrated nanowires again depicting surface water loss and the loss of interlayer water en route to the β phase.

The facile diffusion of water molecules into the β-phase tunnels and the propagation of slip and recrystallization of δ-phase double layers are both assisted by the finite size of the nanowires. Most notably, since the intercalation/deintercalation time $t \approx [d^2/D]$, where D is the diffusion coefficient, shorter diffusion path lengths (d) yield dramatically improved guest insertion/extraction kinetics, enabling water molecules to readily hydrate the β-phase nanowires and initiating the phase transformation to the δ phase. As noted above, the quasi-1D δ and β phases have distinctive charge-ordering patterns; altering the nature of charge fluctuations in the nanowires while retaining the same stoichiometry will permit tuning of metal−insulator transitions. Each of the δ and β phases are characterized by rich phase diagrams including charge-ordered, correlated metallic, and antiferromagnetic insulating states. The methods reported here provide a means to link the phase diagrams at the nanoscale level, enabling sampling of an expansive region of the phase space, and they may further be generalizable to other divalent vanadium bronzes with feasible δ and β polymorphs. The interconversion between two classes of materials exhibiting pronounced metal−insulator transitions will broaden the tunability of active materials for memristors,[27,28] Mott field-effect transistors,[29,30] infrared modulators such as for ballistic missile testing,[31] infrared bolometers, and electrochromic coatings.[32]

In conclusion, we have developed a facile hydrothermal synthetic route for the preparation of quasi-1D δ-phase $Ca_xV_2O_5$ nanowires. Dehydration of the nanowires surprisingly results in reconstruction of the guest V_2O_5 framework to yield a distinctive β-phase tunnel bronze geometry without substantial sintering or degradation of the nanowires. Conversely, mild hydrothermal treatment of β-phase $Ca_xV_2O_5$ nanowires leads to reversion to the δ phase. Such a facile hydration/dehydration-induced interconversion between two prominent quasi-1D structures (accompanied by a change in charge-ordering motifs) has not been observed in the bulk and likely results from the ease of propagation of crystallographic slip processes across the confined nanowire widths for the $\delta \rightarrow \beta$ conversion and the facile diffusion of water molecules within the tunnel geometries for the $\beta \rightarrow \delta$ reversion. Future work will focus on examining single-nanowire electrical transport of the prepared materials.

■ AUTHOR INFORMATION

Corresponding Author
*E-mail: sb244@buffalo.edu.

Notes
The authors declare no competing financial interest.

■ ACKNOWLEDGMENTS

■ REFERENCES

(1) Chernova, N. A.; Roppolo, M.; Dillon, A. C.; Whittingham, M. S. *J. Mater. Chem.* **2009**, *19*, 2526−2552.
(2) Livage, J. *Chem. Mater.* **1991**, *3*, 578−593.
(3) Wang, Y.; Cao, G. *Chem. Mater.* **2006**, *18*, 2787−2804.
(4) Velazquez, J. M.; Banerjee, S. *Small* **2009**, *5*, 1025−1029.
(5) Ueda, Y.; Isobe, M.; Yamauchi, T. *J. Phys. Chem. Solids* **2002**, *63*, 951−955.
(6) Yamauchi, T.; Isobe, M.; Ueda, Y. *Solid State Sci.* **2005**, *7*, 874−881.
(7) Yamauchi, T.; Ueda, Y. *Phys. Rev. B* **2008**, *77*, 104529/104521−104529/104518.
(8) Galy, J. *J. Solid State Chem.* **1992**, *100*, 229−245.
(9) Galy, J.; Lavaud, D.; Casalot, A.; Hagenmuller, P. *J. Solid State Chem.* **1970**, *2*, 531−543.
(10) Withers, R. L.; Millet, P.; Tabira, Y. *Z. Kristallogr.* **2000**, *215*, 357−363.
(11) Patridge, C. J.; Jaye, C.; Zhang, H.; Marchilok, A. C.; Fischer, D. A.; Takeuchi, E. S.; Banerjee, S. *Inorg. Chem.* **2009**, 3145−3152.
(12) Patridge, C. J.; Woo, T.; Jaye, C.; Ravel, B.; Takeuchi, E. S.; Fischer, D.; Ganapathy, S.; Banerjee, S. *Nano Lett.* **2010**, *10*, 2448−2453.
(13) Patridge, C. J.; Wu, T.-L.; Sambandamurthy, G.; Banerjee, S. *Chem. Commun.* **2011**, *47*, 4484−4486.
(14) Goodenough, J. B. *J. Solid State Chem.* **1970**, *1*, 349−358.
(15) Ganne, M.; Jouanneaux, A.; Tournoux, M.; Le Bail, A. *J. Solid State Chem.* **1992**, *97*, 186−198.
(16) Chakraverty, B. K.; Sienko, M. J.; Bonnerot, J. *Phys. Rev. B* **1978**, *17*, 3781−3789.
(17) Kessler, H.; Sienko, M. J. *J. Solid State Chem.* **1970**, *1*, 152−158.
(18) Perlstein, J. H.; Sienko, M. J. *J. Chem. Phys.* **1968**, *48*, 174−181.
(19) Wadsley, A., D. *Acta Crystallogr.* **1955**, *8*, 695−701.
(20) Yamauchi, T.; Ueda, Y.; Mori, N. *Phys. Rev. Lett.* **2002**, *89*, 057002/057001−057002/057004.
(21) Ma, C.; Yang, H. X.; Li, Z. A.; Ueda, Y.; Li, J. Q. *Solid State Commun.* **2008**, *146*, 30−34.
(22) Zhang, X.; Yan, W.; Xie, Y. *Chem. Commun.* **2011**, *47*, 11252−11254.
(23) Zhang, X.; Yan, W.; Xie, Y. *Chem: Asian J.* **2011**, *6*, 3230−3235.
(24) Evans, H. T.; Post, J. E.; Ross, D. R. *Can. Mineral.* **1994**, *32*, 339.
(25) Oka, Y.; Yao, T.; Yamamoto, N. *J. Solid State Chem.* **1997**, *329*, 323.
(26) Oka, Y.; Tamada, O.; Yao, T.; Yamamoto, N. *J. Solid State Chem.* **1995**, *114*, 359.
(27) Driscoll, T.; Kim, H.-T.; Chae, B.-G.; Kim, B.-J.; Lee, Y. W.; Jokerst, N. M.; Palit, S.; Smith, D. R.; Di Ventra, M.; Basov, D. N. *Science* **2009**, *325*, 1518−1521.
(28) Driscoll, T.; Andreev, G. O.; Basov, D. N. *Appl. Phys. Lett.* **2007**, *91*, 062511/062511−062513.
(29) Newns, D. M.; Misewich, J. A.; Tsuei, C. C.; Gupta, A.; Scott, B. A.; Schrott, A. *Appl. Phys. Lett.* **1998**, *73*, 780−782.
(30) Chudnovskiy, F.; Luryi, S.; Spivak, B. In *Future Trends in Microelectronics: The Nano Millenium*; Zaslavsky, A., Ed.; Wiley-Interscience: New York, 2002; pp 148−155.
(31) Richardson, M. A.; Coath, J. A. *Optics Laser Technol.* **1998**, *30*, 137−140.
(32) Whittaker, L.; Patridge, C. J.; Banerjee, S. *J. Phys. Chem. Lett.* **2011**, *2*, 745−758.